Technium Vol. 3, Issue 10 pp.11-22 (2021)
ISSN: 2668-778X
www.techniumscience.com

Numerical Analysis of Gravitational Vortex Chamber

Shahadat Hossain Zehad[*], Sadman Al Faiyaz[**], Md. Redwan Islam[***], Dr. –Ing. Irfan Ahmed[****]

Department of Mechanical Engineering, Bangladesh Army University of Science and Technology, Saidpur, Bangladesh

Corresponding Author: Shahadat Hossain Zehad, shahadathossain01798@gmail.com

Abstract. A rotating mass of fluid is known as vortex and the motion of the rotating mass of fluid is known as vortex motion. Vorticity is the circulation per unit area. In this research simulation of a vortex chamber is to be carried out in ANSYS CFD taking water as fluid domain for generating a water vortex that is capable enough to move a turbine for electricity generation. The CAD modelling of the setup was set down and simulation was done in fine mesh by taking suitable wall function in the model of a cylindrical chamber along with a rectangular channel with a contraction portion at the end of it where good amount of vortex generation was acquired by observing velocity and pressure by setting different parameters. The results shows the pressure and velocity contours with 3D velocity streamline flow and the curve of the velocity and pressure curve shows the decrease of pressure and increase of velocity from inlet to outlet that leads to a decent vortex generation.

Keywords: Vortex, Vorticity, Computational Fluid Dynamics (CFD), Vortex Chamber, Pressure, Velocity.

1. Introduction

Water Vortex is the phenomenon where there is flow of water in a swirl motion that can be represented in cylindrical coordinates with tangential, radial and axial axis. Free vortex always occurs at the water of low head. It helps to accelerate the water flow from slow to high velocity that generates sufficient amount of vorticity for electric power supply. A turbine that is used to harness the power from the generation of water vortex and helps to produce electricity with a generator coupled with the turbine. There are several works which has been done regarding water vortex. As for example, Li et al.9 investigated the flow field of a free surface vortex by employing the particle image velocimetry (PIV) technique. Gordon10, Redy et al.11 and Odgard twelve,13 projected formulas to predict the essential sinking. John et al.14 and bird genus et al.15 summarized the rate field of the free vortex. Zhao et al.16 distributed numerical simulations of the free surface water in an exceedingly barrel with a bottom central passage [1]. By designing a water vortex setup though several CFD simulations, the profile of the best water vortex generation is to be obtained by selecting specific parameters. Electricity generation can be obtained from getting the best vorticity generation from water where the vortex turbines will extract the maximum possible amount of energy produced from sufficient vortex core formation.

2. System Modeling

2.1. Design Model

The design was set and modelled in SolidWorks version 2018 by using basic syntax of a cylindrical vortex chamber and a channel with contraction and the cases which were designed is taken as the fluid

domain by taking the bottom center section of the vortex chamber as the origin from where the design has been produced. The dimensions of the model are given in the table 1.

Table 1. Dimensions of the Setup

Name	Size (m)
Channel Length	1.32
Channel Height	0.3
Inlet Channel Width	0.5
Outlet Channel Width	0.18
Vortex Chamber Diameter	1
Vortex Chamber Height	1
Outlet Diameter	0.15

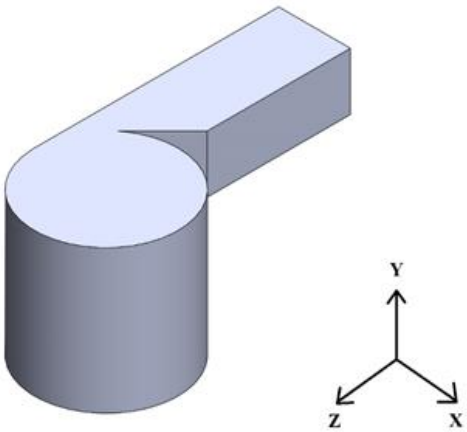

Fig. 1. CAD Model

2.2. Mathematical Model and Governing Equations

The governing equations for the vortex that could be incompressible, viscous, steady and turbulent flow which is satisfied as the continuity equation and the Navier Stokes equation that can be narrated in cylindrical coordinates that goes along with [2][3].

$$\frac{\partial V_r}{\partial r} + \frac{\partial V_z}{\partial z} + \frac{V_r}{r} = 0 \quad (1)$$

$$\partial V_r \frac{\partial V_\theta}{\partial r} + VZ\frac{\partial V_\theta}{\partial z} - \frac{V_r V_\theta}{r} = v\left(\frac{\partial^2 V_\theta}{\partial r^2} + \frac{\partial V_\theta}{r\,\partial r} - \frac{V_\theta}{r^2} + \frac{\partial^2 V_\theta}{\partial z^2}\right) \quad (2)$$

$$V_r \frac{\partial V_r}{\partial r} + VZ\frac{\partial V_r}{\partial z} - \frac{V_\theta^2}{r} + \frac{\partial \rho}{\rho\,\partial r} = v\left(\frac{\partial^2 V_r}{\partial r^2} + \frac{\partial V_r}{r\,\partial r} - \frac{V_r}{r^2} + \frac{\partial^2 V_r}{\partial z^2}\right) \quad (3)$$

$$\partial V_r \frac{\partial V_z}{\partial r} + VZ\frac{\partial V_z}{\partial z} + \frac{\partial \rho}{\rho\,\partial z} = g + v\left(\frac{\partial^2 V_z}{\partial r^2} + \frac{\partial V_z}{r\,\partial r} + \frac{\partial^2 V_r}{\partial z^2}\right) \quad (4)$$

Hence the quality of the above equations are complex enough to solve analytically. Moreover, the presence of multiple domain reads the analytic answer of these equations to a better issue level. And for the, ANSYS CFD was used to solve the answer of those equations [4].

2.3. Numerical Analysis

The parameters of the model which comprises a cylindrical shaped vortex chamber and a rectangular shaped channel with a contraction portion at the outlet of it has been taken for a simulation at necessary boundary conditions. The mesh of the model was taken as fine as possible in tetrahedrons at 500253 no of elements. The aspect ratio of the mesh is 1.94 at skewness of 0.27.

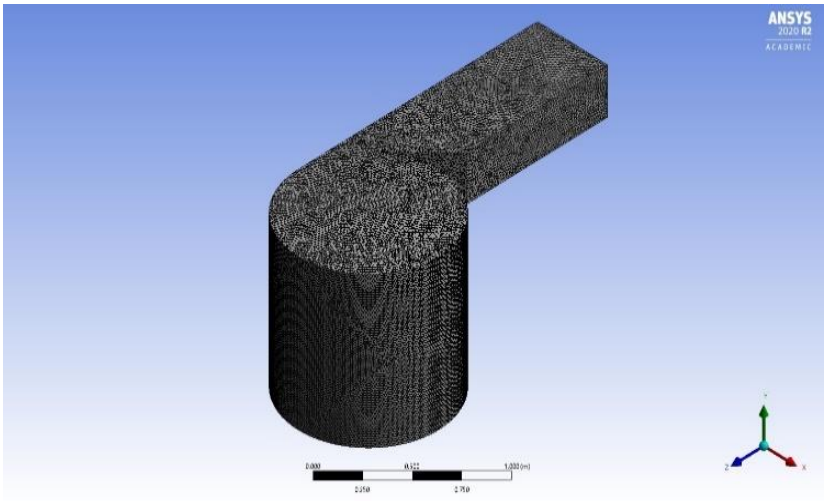

Fig. 2. 3D Generated Mesh

The model has been meshed four times from coarse to fine where it has been observed that the pressure loss coefficient at the last two generated mesh of the model are almost identical. From figure 3 it has been observed that there is almost a negligible difference in the loss of pressure between the last two generated mesh from which it can be concluded that the pressure loss coefficient which defines pressure loss of a definite system or of a part of a system will not vary after the finest mesh has been generated. The pressure loss coefficient has slightly increased due to asymmetric dimensional changes but at a certain level the value loss coefficient becomes almost same. The pressure loss coefficient has been found 2.18 for the finest mesh for this model with an error of 0.0003 which converges the asymptotic range. Hence, the generated mesh is in very good condition [5].

Table 2. Pressure Loss Coefficient and Refinement Ratio of Number of Elements

No. of Elements	**ω_{pt}**	**r**
500253	2.1817	1.12
450236	2.179	1.11
405436	2.176	
492589	2.18171	

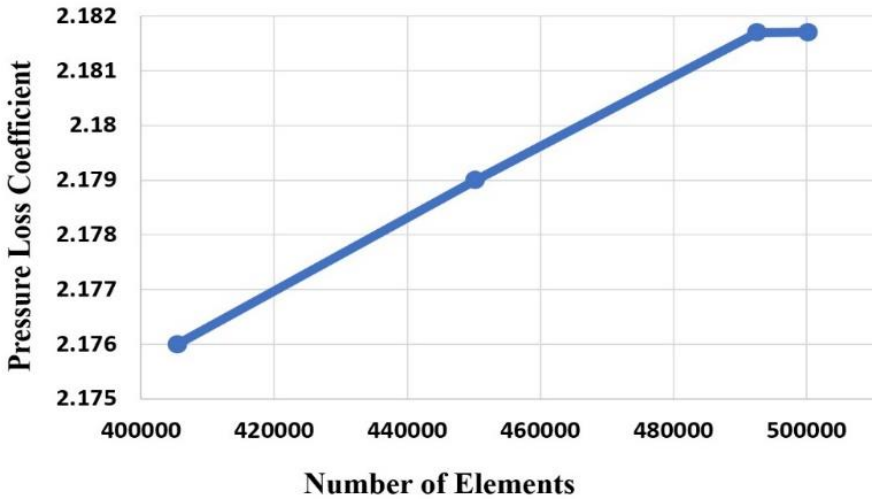

Fig. 3. Pressure loss coefficient over number of elements

Necessary boundary conditions were applied at the inlet and outlet section for the solution of boundary value problem. The model was set by taking fluid domain of water. The flow was run at steady state taking the viscous model at k-epsilon with standard wall function. The inlet was set at 1.64 m/s and outlet as pressure outlet taking gauge pressure of 0 pa selecting all the surfaces as wall with no slip condition. SIMPLE method was used for simulating the model. The setup was run at 10000 no of iterations and the solution was converged passed 1e-4 for the residuals.

Wall functions play an important role in using turbulence modeling. The flow is usually bedded close to the wall, thence turbulence modeling won't be valid during this bedded regime. That is the most reason to use wall functions in turbulent modeling to capture the inner bedded field variables within the flow. The standard wall functions offer moderately correct predictions for the bulk of high Reynolds-number, wall-bounded flows. The non-equilibrium wall performs any extend the relevancy of the wall function approach by as well as the consequences of pressure gradient and robust non-equilibrium [6]. Scalable wall functions make sure that the wall distance used within the wall functions is such $y+\geq 11.126$ regardless of the amount of near-wall grid refinement. This worth of y+ marks the intersection of the linear and exponent rate profiles [7]. The highest wall yplus value was obtained for this model was 3.50e+2 in the channel wall and 1.117e+3 in the vortex chamber wall for both standard and scalable wall functions.

3. Results and Discussions

The streamlines had been shown in the given figures 4 and 5 where the flow of the stream paths are given in the direction of flow. This velocity streamline illustrates the conical-shaped formation of the streamlines which is the vortex formation. As the streamline descends gradually, the area of the air cone gets decreased. The streamlines move radially to the bottom of the chamber where the stream paths are not symmetric at all. The color scales represent the magnitude of the velocity from which the velocity of the streamlines can be known at different positions.

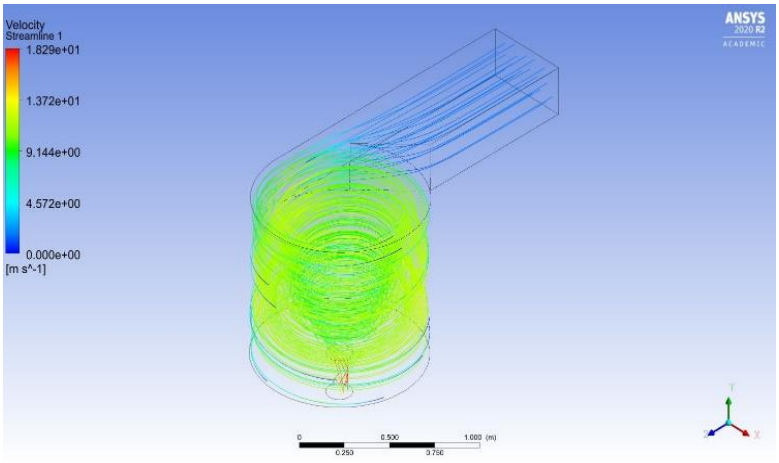

Fig. 4. Velocity Streamline Flow (Isometric View)

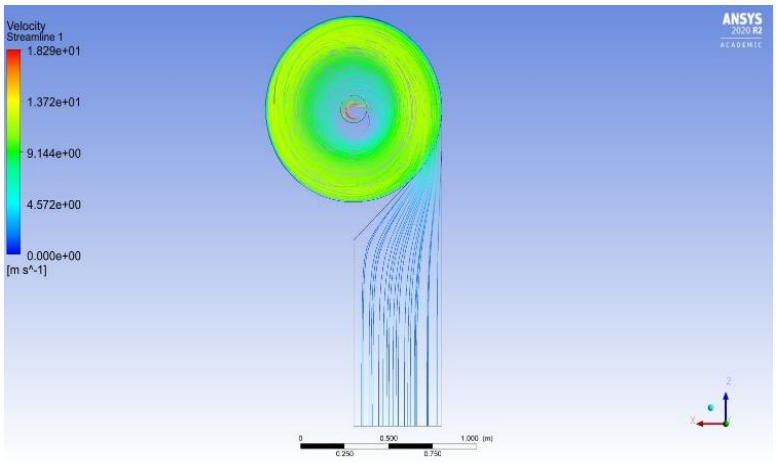

Fig. 5. Velocity Streamline Flow (Top View)

From figures 6, 7, and 8 the velocity contours of the vortex chamber at different positions are observed. The contour plane at the XY section has been rotated from 0^0 to 45^0 and 90^0 respectively that is from the neutral position of the plane at 0^0, the plane has been rotated to two more degrees to observe the velocity profile of the vortex chamber. Here, the velocity in the chamber increases as the flow of water reaches the outflow pipe. There is an air-cone formation observed from the blue-colored velocity contour of the conical shape.

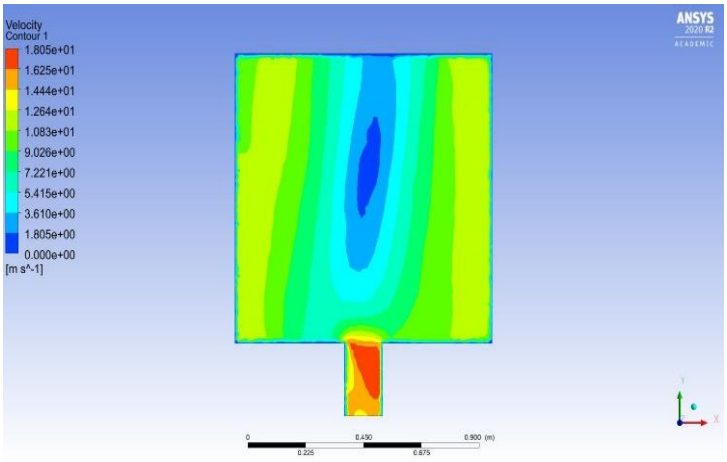

Fig. 6. Velocity Contour of XY Plane at 0 Degree

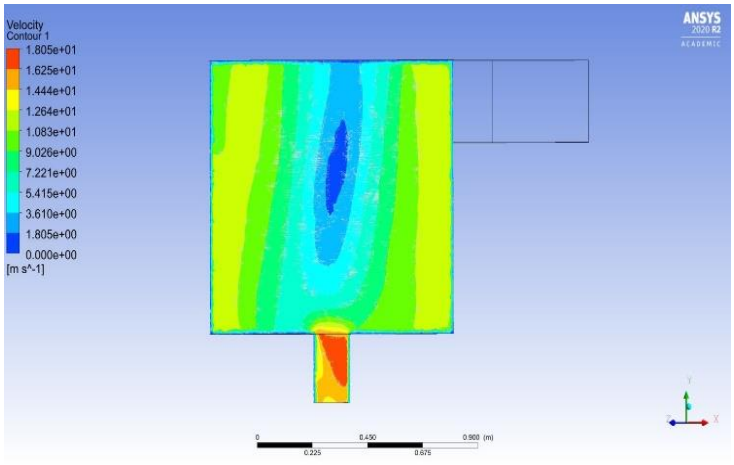

Fig. 7. Velocity Contour of XY Plane at 45 Degree

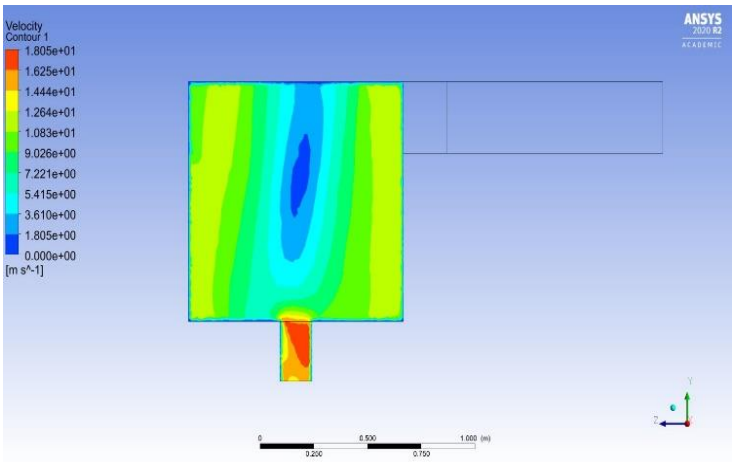

Fig. 8. Velocity Contour of XY Plane at 90 Degree

More clear image of the vorticity generation along with its position can be seen from the pressure contour plots showed from the top view given in figures 9, 10, 11, 12, and 13 based on different heights respectively along the ZX plane. From the figures, it is observed that the air-core formation from the top of the chamber to the bottom of the chamber is decreasing gradually. That helps to understand the structure of the core is conical and the position of the core varies with the height of the chamber respectively [8].

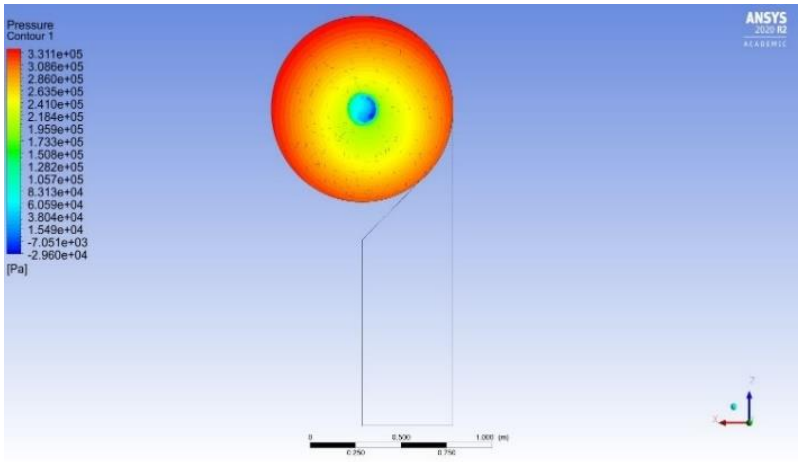

Fig. 9. Pressure Contour from bottom at 0%

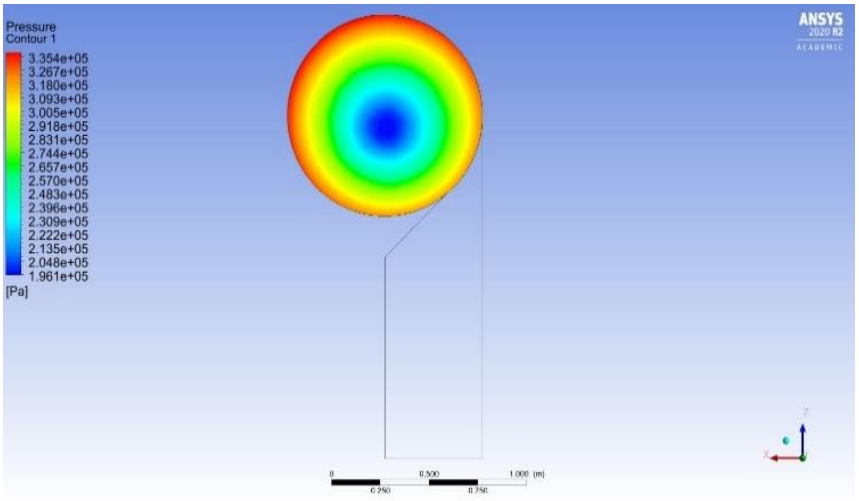

Fig. 10. Pressure Contour from bottom at 25%

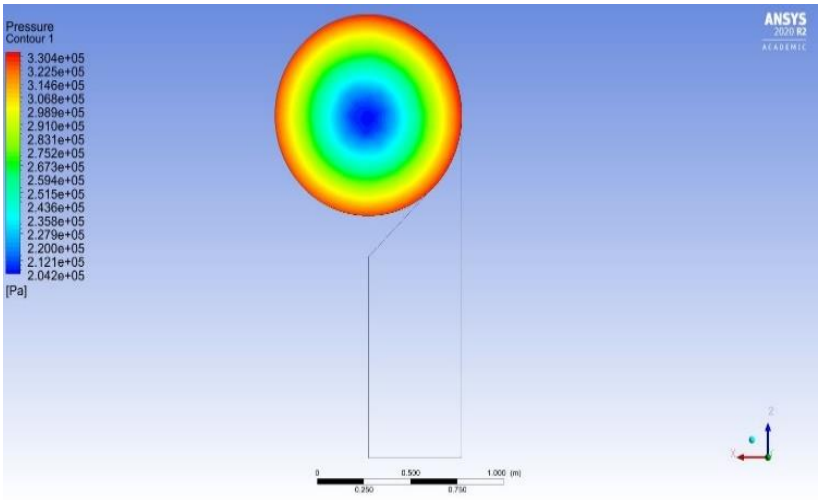

Fig. 11. Pressure Contour from bottom at 50%

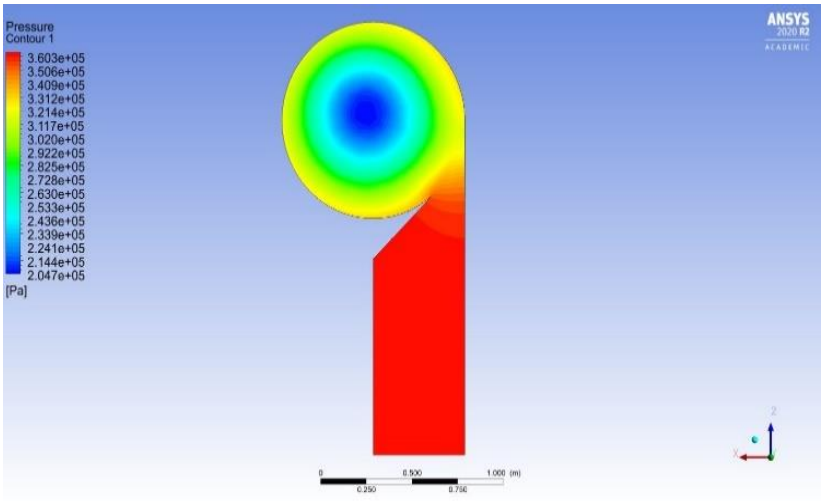

Fig. 12. Pressure Contour from bottom at 75%

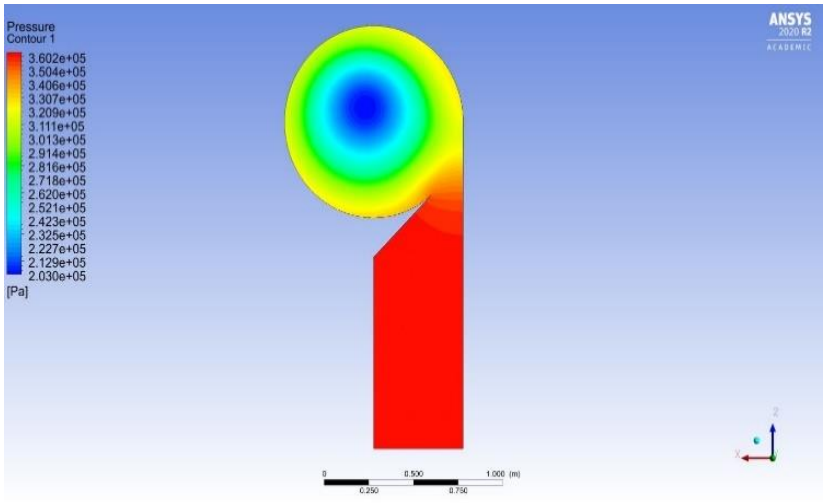

Fig. 13. Pressure Contour from bottom at 100%

The vortex formation of the model is displayed respectively in the form of lambda-2 criterion, pressure, and velocity in figures 14, 15, and 16 where the best vorticity generation that has been obtained from this model. The lambda-2 criterion vortex formation is shown in figure 14 which merely considers the definition of the scalar lambda-2 and the way turbulent structures are often unreal by correct iso-surfaces of lambda-2 (like for the Q criterion). This is often outlined as the second (in magnitude) eigenvalue of the matrix [9]. Jeung and Hussain explained that the lambda-2 criterion uses a second-order tensor Ω2+S2 that describes a vortex.

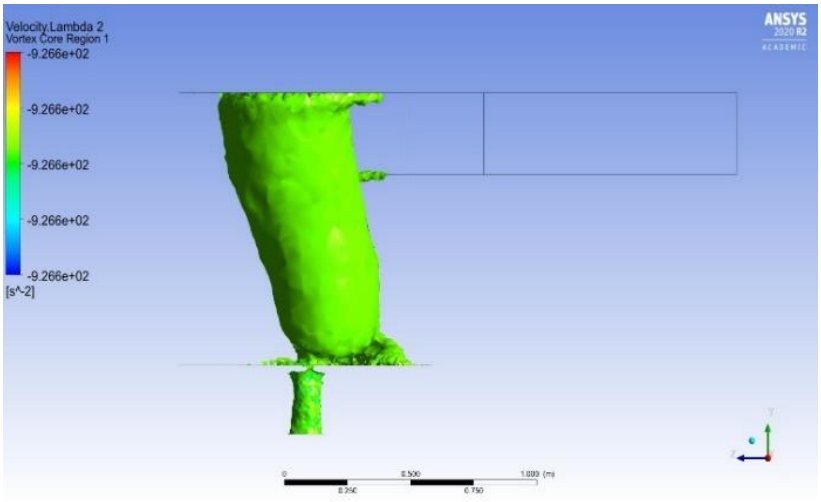

Fig. 14. Lambda-2 Criterion Vortex Formation

From the figure 15, the pressure gradient can be shown as

$$\frac{dP}{dr} = \Omega^2 r \qquad (\mathbf{5})$$

That is at the vicinity of the line of core for isolated axisymmetric vortices and an estimation when the vortices are plunged in the pressure gradient which is generated by other flows such as nearby vortices.

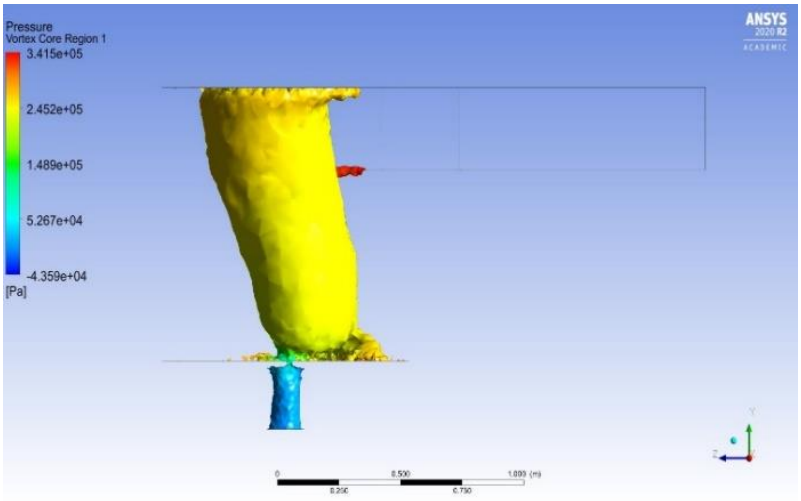

Fig. 15. Pressure Vortex Formation

In the figure 16 the velocity of the vortex core is shown, since there is no velocity from the air-core, thus azimuthal velocity decreases. Rankine vortex can be defined as the simplest vortex where vorticity is zero at the outside and remains constant at vortex core. [10].

$$v_\theta = \frac{1}{r\left(1 - e^{r^2}\right)} \qquad (6)$$

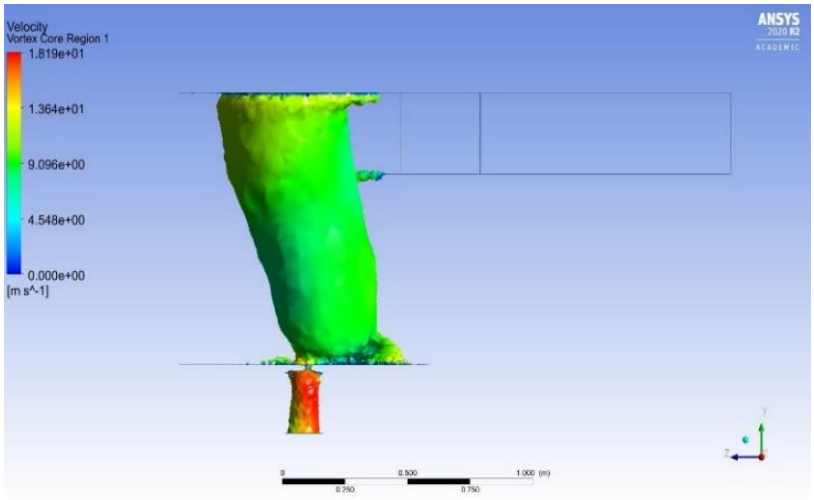

Fig. 16. Velocity Vortex Formation

The above figures 14, 15, and 16 show the position of the vortex formation is not straight and the formation is getting deviated from its origin as the flow approaches the outlet section.

To get a good vortex formation, there will be a pressure difference from the inlet to the outlet section. The static pressure of the channel decreases as the velocity reaches at maximum in the contraction section of the channel which is seen from figures 17 and 18 respectively. The total pressure has been increased a little at the contraction section of the tunnel. When the tunnel is about to get contracted at the outlet region, the fluid particle hits at the walls of the contracted region where the velocity of the fluid particle becomes zero which is the stagnation region of the tunnel thus giving an increase in total pressure in the

stagnation region and a corresponding decrease in areas around that contracted portion of the tunnel. In the channel section, the curve has been shown by plotting a line from the inlet to the outlet at the middle section from the y-axis and a bit off-centered from the x-axis for showing the velocity at the middle of the contraction portion. The inlet of the channel is at -1.7m and the outlet at -0.4m along the z-axis respectively.

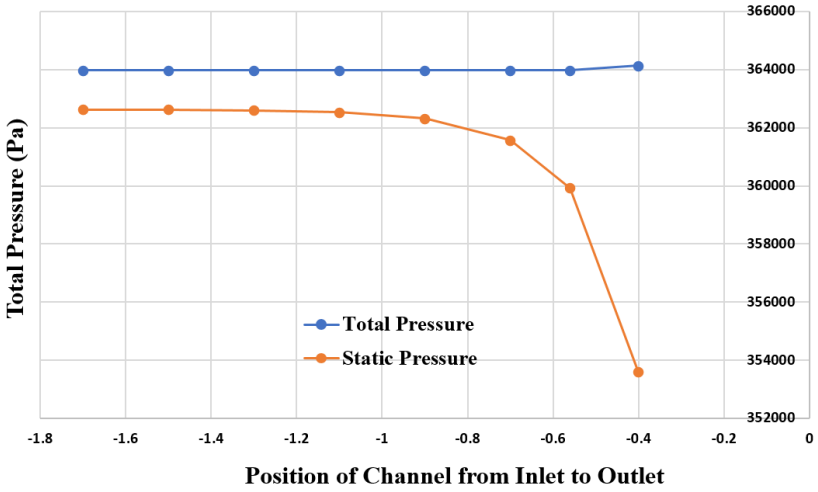

Fig. 17. Pressure Curve of Channel

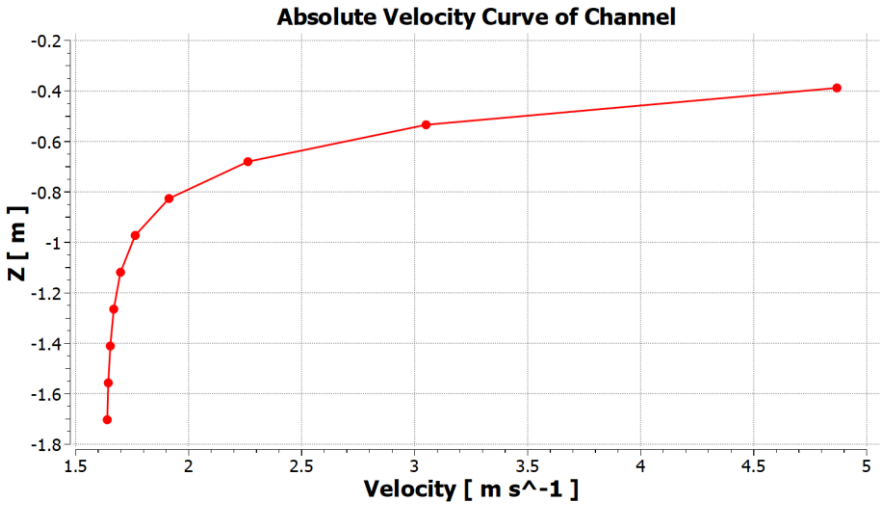

Fig. 18. Absolute Velocity Curve of Channel

As in the Vortex Chamber, both the total and static pressure from the top to bottom gradually decreases with the increase of velocity given in figure 19 and figure 20 respectively. This shows the flow of the fluid moves from the top of the vortex chamber to the outlet section from where the fluid comes out. Hence the air-core is not symmetrical, the velocity curve deviates at a certain position at decreasing value and then accelerates towards the bottom of the chamber. The curve has been shown by plotting a line through the center of the vortex chamber along the y-axis where the upper limit is 0.85m and the bottom limit at 0m.

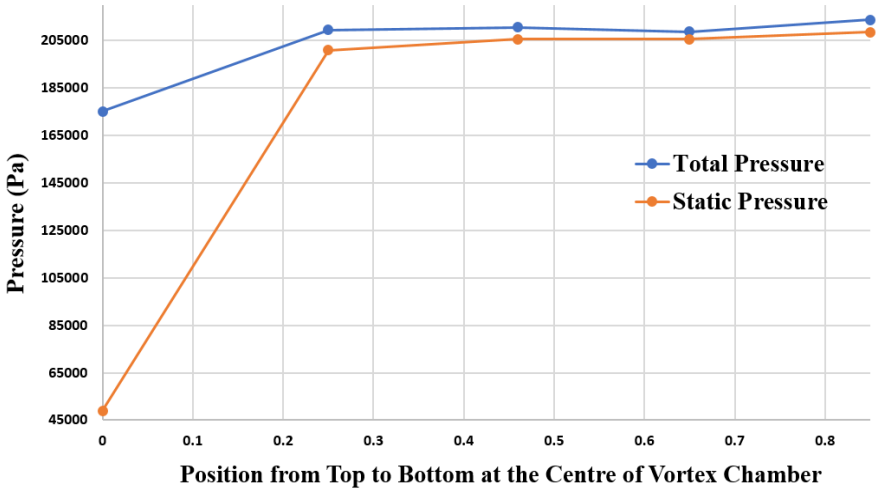

Fig. 19. Pressure Curve of Vortex Chamber

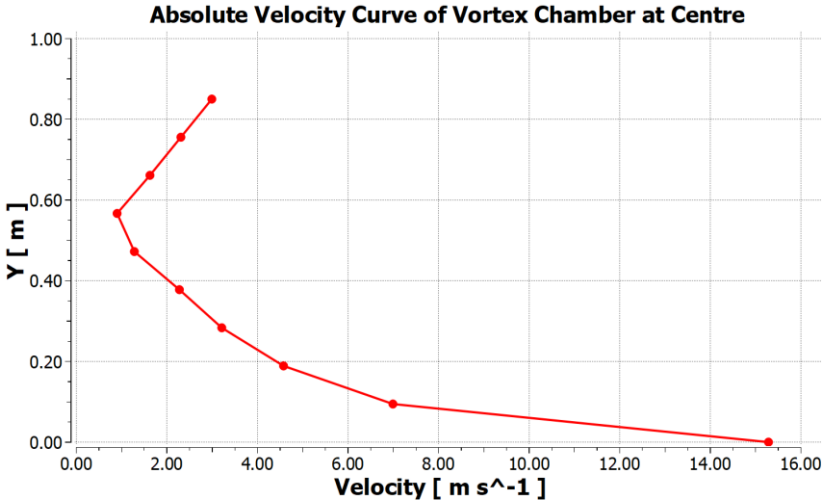

Fig. 20. Absolute Velocity Curve of Vortex Chamber

The curve has been plotted according to the line which is taken at the section of channel and vortex chamber which has been calculated by setting the origin point at the bottom center position of the vortex chamber.

4. Environmental Impact

Because of the environmental, technical, and economic benefits of hydropower, there are some useful values for water in these aspects. Water has a large amount of availability and extracting energy from water through vortex generation causes no harm to no environmental pollution. Micro-hydro power plants can be set through the vortex generation of water to produce electricity generating no pollution to the environment and as well as no aquatic animals will be harmed. As water is a vital source of renewable energy, it can be used in low heads and even at high heads using a vortex generation setup for the generation of electricity in a comparatively less expensive way.

5. Conclusions

A numerical analysis on the gravitational vortex chamber taking water as the fluid domain was supervised in this research. As it is very difficult to crack through the complex analytical equations of vortex formation, a simulation was done for the solution. However, the vortex formation would be straight if the analytical equations could be solved properly whereas the simulation result showed the deviation of the vortex core from its origin. The simulation was carried out by following proper methodology and using Richardson extrapolation method. The solution of the simulation was converged at 1e-4 in steady-state condition where the pressure and velocity at the vortex chamber and as well as at the channel section was inversely proportional to each other. The precision level of vortex formation could be more if the solution of all the residuals converged at 1e-6 and also if the model could be done in the structural mesh as it defines more accuracy than the mesh with tetrahedrons. Besides, the wall yplus value was high as no boundary layer was set while meshing the model. The value of wall yplus could be more less if the boundary layer was applied adequately. The vorticity obtained from the simulation result depends on the inlet section of the channel, vortex chamber, outlet section, and other parameters. More research will be carried out to analyze the vortex formation by modeling different geometries and setting different parameters. All of the tests could not be done as this is the very first step. A lot of emphases has been put on this research because depending on the nature of vortex formation, power can be produced.

References

[1] S. Wanchat and R. Suntivarakorn*: Preliminary Design of a Vortex Pool for Electrical Generation, *Journal of Computational and Theoretical Nanoscience*, January 2011 DOI: 10.1166/asl.2012.3855.

[2] Sagar Dhakal, Ashesh Babu Timilsina, Dinesh Fuyal, and Nagendra Amatya: Mathematical modeling, design optimization and experimental verification of conical basin: Gravitational water vortex power plant, *World's Largest Hydro Conference*, Portland, 2015.

[3] Ying-kui Wang, Chun-bo Jiang, and Dong-fang Liang: Investigation of air-core vortex at hydraulic intakes, *9th International Conference on Hydrodynamics*, Shanghai, China, 2010.

[4] Ansys Fluent 12.0 User Guide, *ANSYS Inc.*, April 2009.

[5] Roache, P.J., K. Ghia, and F. White: Editorial Policy Statement on the Control of Numerical Accuracy, *ASME Journal of Fluids Engineering*, Vol. 108,No. 1., March 1986, p. 2.

[6] B.E. Launder and D.B. Spalding: The Numerical Computation of Turbulent Flows, *Computer Methods in Applied Mechanics and Engineering*, 3:269-289, 1974.

[7] H.Grotjans & F.R.Menter: Wall functions for industrial applications, *In Proc. of CFD'98, ECCOMAS*, 1(2), Papailiou KD (Ed.). Wiley: Chichester, UK, 1112–1117, (1998).

[8] Shahadat Hossain Zehad, Sadman Al Faiyaz, Irfan Ahmed, and Ahmed Masruk Raihan: A Comparative Numerical Analysis for Vortex Generation on Different Geometries, *Lecture Notes in Engineering and Computer Science: Proceedings of The World Congress on Engineering*, 7-9 July, 2021, London, U.K., pp262-267, ISBN: 978-988-14049-2-3.

[9] Jinhee Jeong and Fazle Hussain: On the identification of a vortex, *Journal of Fluid Mechanics*, Volume 285 , 25 February 1995 , pp. 69 – 94, DOI: https://doi.org/10.1017/S0022112095000462.

[10] Jiajia Li and Pablo M. Carrica*: A simple approach for vortex core visualization, *IIHR-Hydroscience and Engineering*, The University of Iowa, Iowa City, IA 52242, USA.